Miniature Intraoral Robot (MIR) for Minimally Invasive Tooth Preparation

Yukiko Tomooka, Carina Schmidt, Jenni Hjerppe, Marc Balmer, Ronald Jung, Raphael Mohler, Ahmet Yildiz, Murali Karnam, Manuela Eugster, and Georg Rauter, *Member, IEEE*

***Abstract*—Dental restorations are used to replace the loss of natural tooth structure for medical reasons, to restore function, or to improve aesthetics. For this purpose, the affected teeth are manually prepared to provide adequate space for the dental restoration. The outcome of tooth preparation depends largely on the skills and experience of the dentists. To improve consistency, predictability, and reduce invasiveness, we developed a Miniature Intraoral Robot (MIR). The MIR was designed to be mounted inside the mouth and actuated by remotely placed motors via flexible shafts. This paper presents the workflow, requirements, concept, prototyped MIR design, and its performance evaluation in positioning accuracy and grinding of resin and dental hybrid ceramic workpieces on the test bench. Actuation via flex shafts successfully achieved delay-free 1:1 torque transmission across various speeds and frequencies. In open-loop control, the prototype successfully demonstrated circular path-following motions with and without grinding. The positioning error without grinding resulted in an average absolute positioning error of 0.18 mm. The deviation of the actual ground surface from the planned ground surface resulted in an average absolute error of 0.16 mm. These results suggest that the prototype reached the required order of magnitude for dental interventions despite the sole reliance on remotely placed motor encoders without any position sensors inside the MIR's joints.**

***Index Terms*—Minimally invasive, parallel robot, dental restoration.**

Received 23 August 2025; revised 19 December 2025 and 20 February 2026; accepted 1 April 2026. Date of publication 9 April 2026; date of current version 5 May 2026. This article was recommended for publication by Associate Editor S. Wang and Editor F. Ficuciello upon evaluation of the reviewers' comments. This work was supported in part by Innosuisse under Grant 101.453 IP-LS; in part by Camlog Biotechnologies GmbH; in part by the Investment Fund of Prof. Ronald Jung, Clinic of Reconstructive Dentistry, Center for Dental Medicine, University of Zürich; in part by the Federal Commission for Scholarships for Foreign Students (FCS) of the Swiss Confederation (Swiss Government Excellence Scholarships) under Grant 2021.0170/Japan/OP; and in part by the Werner Siemens Foundation (projects: Minimally Invasive Robot-Assisted Computer-Guided Laserosteotome (MIRACLE*II*)). *(Murali Karnam, Manuela Eugster, and Georg Rauter are co-last authors.) (Corresponding author: Yukiko Tomooka.)*

Yukiko Tomooka, Carina Schmidt, Murali Karnam, and Georg Rauter are with the BIROMED-Lab, Department of Biomedical Engineering, University of Basel, 4123 Allschwil, Switzerland (e-mail: yukiko.tomooka@unibas.ch).

Jenni Hjerppe, Marc Balmer, and Ronald Jung are with the Clinic of Reconstructive Dentistry, Center for Dental Medicine, University of Zürich, 8032 Zürich, Switzerland.

Raphael Mohler and Ahmet Yildiz are with Camlog Biotechnologies GmbH, 4053 Basel, Switzerland.

Manuela Eugster is with the BIROMED-Lab, Department of Biomedical Engineering, University of Basel, 4123 Allschwil, Switzerland, and also with the ARTORG Center, University of Bern, 3008 Bern, Switzerland, also with the Department of Neurosurgery, Inselspital (Bern University Hospital), 3010 Bern, Switzerland.

This article has supplementary downloadable material available at https://doi.org/10.1109/TMRB.2026.3682629, provided by the authors.

Digital Object Identifier 10.1109/TMRB.2026.3682629

I. Introduction

DENTAL restoration is commonly required to address medical or aesthetic needs in dentistry. The most prevalent conditions that require such treatment are the loss of tooth structure due to caries or fractures. These defective conditions are typically treated with partial or full restoration of the tooth structure, such as a filling, crown, or veneer. Dental restoration involves the removal of the decayed tooth part and sometimes also the removal of healthy tooth structure in order to generate sufficient space for restoration material placement. For a crown restoration, a circumferential tooth preparation is performed to create a tapered shape that allows the insertion of a restoration. The typical workflow for a dental restoration involves multiple clinical and laboratory steps (Fig. 1 top row). After a consultation, dentists manually prepare the tooth by removing the necessary volume of tooth substance using electric or pneumatic handpieces with dental diamond burs. An intraoral scan of the tooth is taken and used as a template by the dental technician to design and fabricate a fitting restoration. The subsequent restoration fabrication process is time-consuming and involves either an additional patient visit or waiting time. There are two main restoration fabrication methods: (1) laboratory fabrication by a dental technician and (2) chair-side fabrication by a dentist. Laboratory fabrication requires the patient to visit the dentist another day to cement the restoration. A chair-side fabrication requires additional waiting time during the appointment to complete the manufacturing, and the restoration is then cemented by the dentist. The restoration can be fabricated only after the tooth preparation because the tooth is prepared manually by dentists and the final shape of a prepared tooth cannot be accurately predicted. Therefore, patients must revisit the dentist for restoration placement or endure a long waiting time to avoid additional visits.

Conventional crown preparations are often invasive, requiring extensive removal of healthy tooth substance to accommodate full-coverage restorations. During the tooth preparation, dentists have to visually evaluate the amount of tooth substance removed. Visual inspection alone does not provide adequate feedback regarding the amount of material removed and may result in the removal of more tooth substance than necessary. It has been reported that traditional crown preparations may require the removal of up to 75.6 % of the tooth structure to create sufficient space for the final restoration [1], [2]. Minimally invasive partial restoration has emerged as a newer technique that focuses on preserving as much natural tooth structure as possible by restoring only the damaged portion of the tooth, rather than covering the entire surface. A recent review article showed that teeth restored with conventional crown restorations seem to exhibit more biological complications in short- to mid-term follow-ups compared to

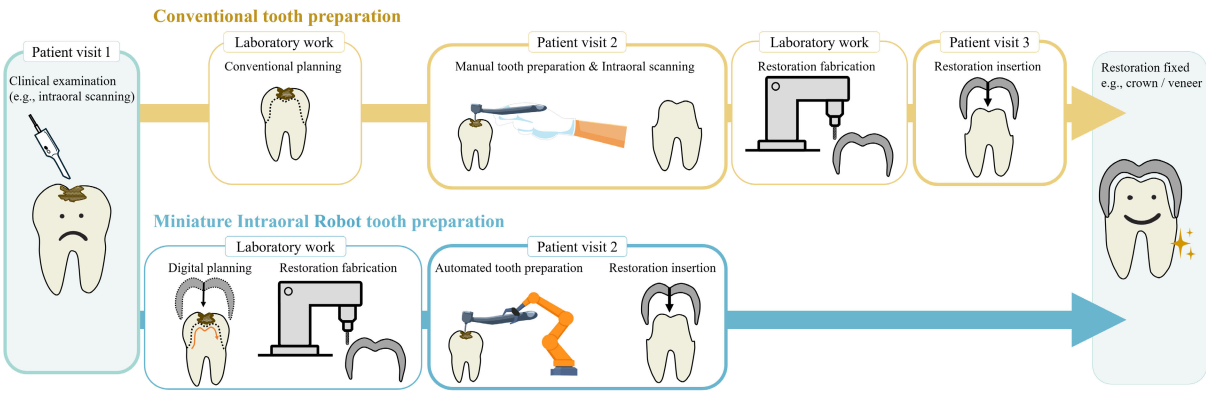

Fig. 1. Workflow comparison between the current manual workflow (top row) and our proposed alternative workflow (bottom row). The existing workflow for tooth restoration involves at least three patient visits at the dentist. Manual tooth preparation is carried out in the second visit (top row). Our proposed alternative workflow requires fewer visits to the dentist. The tooth is accurately prepared according to a digital plan by a robot, and a pre-fabricated restoration is inserted during the same visit (bottom row).

teeth restored with minimally invasive partial restorations [3]. Another biological cause of restoration failure could be heat-related trauma generated during tooth preparation, which can lead to loss of pulp vitality [4], [5]. The amount of heat generated during the tooth preparation procedure depends on several factors, including the applied force, spindle speed, type of bur, duration of continuous grinding, and the effectiveness of the cooling technique. These parameters have to be selected by dentists on site while performing delicate tasks requiring high precision. Therefore, tooth preparation is a procedure that requires high skills, combining precise bur motions and clinical judgment. The clinical outcome of tooth preparation is highly dependent on the skill of dentists, leading to variability in clinical outcomes.

To achieve more consistent and predictable results while reducing the invasiveness of treatments, we aim to automate tooth preparation using robotic systems. We propose an automated tooth preparation workflow consisting of several key steps (Fig. 1 bottom row). During the first visit to the dentist, the patient undergoes a dental examination, including an intraoral scan. Subsequently, digital planning of the ideal tooth preparation and the fabrication of the restoration are performed in the laboratory without the presence of the patient. In the patient's second visit, the automated tooth preparation is carried out according to the digital plan, and subsequently, the pre-fabricated restoration can be inserted. We expect that this approach enables a fully integrated digital workflow, minimizing deviations between the planned and executed preparation. As a result, the volume of tooth substance removal can be optimized, and the restoration can be prefabricated and inserted immediately after automated preparation. This automated approach is expected to reduce the invasiveness of tooth preparation and the number of clinical appointments, thereby improving efficiency and lowering costs.

Existing approaches for tooth preparation that incorporate digital planning involve analog mechanical guidance techniques or automated robotic tooth preparation. Analog mechanical guidance devices, such as FirstFit (Henry Schein, USA) and DigitalPrep [6], use 3D printed guides to manually remove layers of the tooth in a step-by-step manner. These 3D printed tooth reduction guides allowed accurate preparation, preserving natural tooth structure. However, preparation time using these guidance devices was not reported [7], [8].

Robotic preparation approaches are often based on large and stiff robotic arms that operate based on the absolute position. Such a rigid-robot approach typically consists of a serial robotic arm with rigid links and an end-effector holding a dental handpiece, while an external mechanical or optical tracking system provides patient position feedback to compensate for positioning inaccuracies resulting from patient movements.

For example, the feasibility and accuracy of automated tooth preparation for veneers were evaluated using phantom teeth and serial robots [9], [10]. Accuracy comparisons between automated and manual approaches yielded mixed results in these studies. Improved accuracy was demonstrated using robot-assisted tooth preparation compared to free-hand preparation in [9], while robot-assisted tooth preparation exhibited slightly lower accuracy in [10]. Sun et al. proposed optimization methods for the robot's trajectories [11], [12], postures [13], and grinding parameters [12], [14]. They investigated the influence of the robot's trajectories, postures, and grinding parameters on the feasibility of tooth preparation and the grinding results using isolated human teeth fixed to a test bench or a phantom head.

Beyond laboratory and phantom-based studies, two robotic systems have been evaluated on human patients in clinical trials. Perceptive (Massachusetts, USA) has been developing a robotic system to automate tooth preparation. Their preliminary preprint article reported the world's first in-human study of a semi-automated robotic tooth preparation system, conducted in Barranquilla, Colombia, with six participants undergoing tooth preparation for crowns. The system consisted of a serial robot arm with a dental handpiece and a specialized suspension system used to support the robot's weight and rigidly couple the robotic system to the patients' own dentition. This suspension system was employed to compensate for the minor patient movement without the need for optical motion tracking. In the shape analysis that compared the planned and actual tooth geometries, the deviation of root mean square (RMS) was below 0.050 mm when best-fit alignment was performed using only the prepared surfaces alone. When alignment was based on the occlusal surfaces of adjacent teeth, the deviation was below 0.110 mm [15]. This robotic system from Perceptive has neither been approved in the USA nor the EU [16] as of January 2026.

A dental robot from Lupin Dental SAS (Montpellier, France) underwent a post-market clinical study in Pune, India, involving tooth preparation of 52 teeth in 12 participants for laminate veneers. The system used a serial robot arm with a dental handpiece and an optical tracking system with a response latency of less than 100 ms. Patient movement was tracked using a 3D-printed, patient-specific splint with tracking markers, which was also used to maintain the opening of the mouth. The RMS errors between the planned and actual prepared tooth geometries centered on 0.15 mm, and the maximum error of 0.865 mm was observed [17]. This system has not yet entered the markets in the EU or the USA as of February 2025 [18].

Challenges with serial robotic devices include their bulky structure, which can obstruct the dentist's workspace. Furthermore, achieving high accuracy remains a primary challenge due to the potential patient motion during procedures. Patient motion can directly affect the robot's positioning accuracy with respect to the patient's teeth, since the robot operates in a room-fixed workspace in which relative motion of the patient can occur. Consequently, an external motion tracking system is essential to register the robot's position with respect to the patient. However, using an external motion tracking system introduces latency since the system must first detect the patient's motion, process the data, and then generate and transmit appropriate control commands to the robot before relative motions can be compensated. This latency leads to a delay between the actual motion of the patient and the robot's corrective action by design, potentially affecting accuracy and safety. To our knowledge, there was no report that quantitatively assessed the influence of patient movements on the accuracy of the existing robotic systems for tooth preparation. Thus, it remains unclear to what extent patient movement can be tolerated while still allowing currently available systems to achieve the required sub-millimeter accuracy for tooth preparation.

To overcome the positioning challenge of systems that rely on absolute positioning and have to compensate for relative patient movements, an alternative approach is to use small robots mounted directly on the target tissue (i.e., the teeth), allowing high relative positioning accuracy. Such a small robot concept was proposed for root canal treatments by Dong et al., however, its feasibility and performance of root canal treatments remain unclear [19], [20], [21]. To our knowledge, small robotic systems for tooth preparation have only been proposed in patents [22], [23], [24], [25], [26], [27] with no reports available on their actual development or implementation.

While most existing robotic tooth preparation approaches use a dental handpiece with mechanical burs for tooth preparation, Yuan et al. proposed an automatic tooth preparation robot equipped with an ultra-short wavelength laser. The system was evaluated using a phantom head, and tooth preparation was demonstrated in 15 molars with a shape error of 0.05 mm - 0.17 mm [28]. Another example aiming at using a laser for hard tissue manipulation is a miniature robot prototyped for minimally invasive laser osteotomy, which demonstrated an average positioning accuracy of 0.069 mm. This miniature robot was designed to attach to a target tissue and connect to external components with a flexible channel to allow accurate relative positioning of a laser relative to the patient [29], [30]. The local attachment of the miniature robot, combined with flexible connections, allowed mitigating the propagation of mechanical disturbances between external components and internal components to be placed inside the body [31], [32]. However, laser-based tooth preparation potentially has several drawbacks, including longer preparation times and the production of unpleasant odor [33].

To address the challenges associated with the use of a serial robot, specifically the need for high absolute positioning accuracy and the difficulty of maintaining safety and accuracy during patient movement, we propose a patient-mounted miniature intraoral robot (MIR). Our initial conceptual idea is illustrated in Fig. 2. The MIR was designed to be mounted inside the patient's mouth using a mechanical fixation block (i.e., bite block). The relative fixation of the robot by the bite block to the target tissue should allow automating tooth preparation while ensuring the relative positioning between the robot and the patient. Based on the prototype of the miniature robot for laser osteotomy previously presented with high positioning accuracy [29] and our initial idea of the miniature intraoral robot (Fig. 2), the robot design was adapted for the preparation of teeth with mechanical burs, and its performance was evaluated on the test bench.

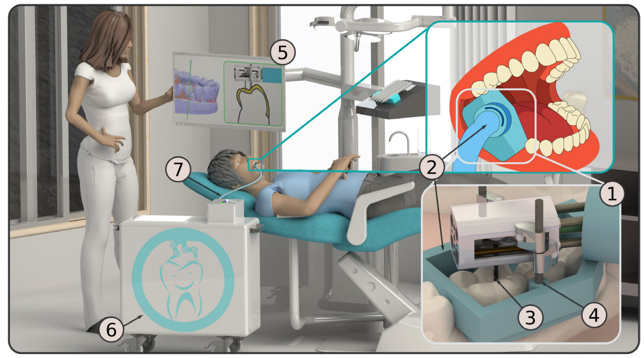

Fig. 2. Initial idea of the miniature intraoral robot. The tooth preparation is carried out by the miniature intraoral robot (MIR) (1). This robot can be mounted inside the patient's mouth using a personalized bite block (2) and precisely guides a dental bur to perform the preparation (3). The robot has a rigid connection to a personalized bite block, allowing accurate positioning of a dental bur for tooth preparation (4). The dentist can control and supervise the process (5). Bulky or heavy components of the robot are located next to the dental chair (6). All components required for tooth preparation (e.g., rotation of bur and cooling) inside the mouth are transmitted through a flexible supply channel (7).

This paper presents the following main contributions:

1) The MIR's requirements, concept, and workflow.
2) The MIR's prototype design and implementation.
3) The MIR's positioning accuracy and grinding performance evaluation with resin and dental hybrid ceramic workpieces on the test bench.

II. Requirements and Concept

In this section, requirements and the concept of the miniature intraoral robot (MIR) to automate tooth preparation, such as crown and veneer preparation, are described.

A. Requirements

Intraoral robots for tooth preparation must satisfy challenging requirements attributed to the operating environment within the patient's oral cavity.

Safety, cleanliness, and sterilization are critical requirements for medical devices. Depending on the intended use, risk classification, and the level of contact with the patient, the device must either be enclosed within a biocompatible housing that can be cleaned easily or be designed to withstand a validated sterilization process, such as steam. For example, devices used in dentistry, such as handpieces, often require cleaning and autoclaving. Cleaning is required to remove debris and organic contaminants. Autoclaving typically involves saturated steam

TABLE I
MINIATURE INTRAORAL ROBOT'S REQUIREMENTS

Robot's requirements			**Reference and relevant information**
Degree of Freedom (DoF)		3 translational DoF of bur + bur rotation	abutment tooth preparation without undercuts
Workspace	X (mesiodistal direction)	11 mm + bur diameter	Maximal mesiodistal tooth diameter [34], [35]
	Y (buccolingual direction)	11 mm + bur diameter	Maximal buccolingual tooth diameter [34], [35]
	Z (cervicoincisal direction)	11.7 mm + gingival recession (0 mm - 4 mm)	Maximal cervicoincisal tooth length [34], [35] and gingival recession [36]–[39]
Robot size	X (mesiodistal direction)	No strict requirements	No strict requirements
	Y (buccolingual direction)	around 30 mm or smaller	Commercial bite block width: approximately 25 mm
	Z (cervicoincisal direction)	17 mm - 32 mm at 2nd molar	Active mouth opening of 75% participants [40]
Overall positioning accuracy		0.12 mm	Space between crown and tooth for cementing [41]
Grinding force		Around 1 N - 3 N, below 5 N	Literature on grinding force measurements by dentists [42], [43]

at high pressure and temperature (commonly 121 °C or 134 °C). Therefore, a medical device that requires autoclaving has to withstand the high temperatures and humidity.

Tooth preparation involves the removal of tooth substance, followed by shaping the remaining tooth structure to accommodate dental restoration such as a crown or veneer (e.g., 0.8 mm - 1 mm circumferential tooth substance removal in crown preparation). Shaping appropriately tapered axial walls (e.g., recommendation 3 °C - 6 °C for crown preparation) without undercuts is important to enable proper insertion and retention of the restoration [41]. A controlled luting agent space (i.e., a marginal gap between the prepared tooth and a restoration) is also essential to facilitate the flow and uniform distribution of the luting agent, ensuring adequate seating, adhesion, and long-term stability of the restoration [44]. Several studies report that gaps between 50 μm and 120 μm are clinically acceptable, whereas others recommend maintaining gaps below 100 μm [45]. Inappropriate luting agent space, i.e., either excessively thin or thick luting agent, can lead to reduced clinical performance. For example, excessively thin luting agents can lead to incomplete seating, point contact stress, or insufficient distribution of luting agent. However, a thicker luting agent layer can introduce internal stress during polymerization, reduce the mechanical strength, and retention due to lower adhesive strength across a wider luting agent volume [44]. In addition, an excessively large luting agent space unnecessarily increases the invasiveness of tooth preparation and can compromise the marginal integrity of the restoration, leading to microleakage, secondary caries, and periodontal inflammation.

Robots intended for intraoral use must comply with specific anatomical constraints that influence their design and functionality. Anatomical constraints include the mouth opening that defines the maximum allowable dimensions of the device. Active mouth opening measured at the Clinic of Reconstructive Dentistry, University of Zürich, in Switzerland showed a mouth opening range of 36 mm - 67 mm at the central incisor (99 participants), 22 mm - 48 mm in the first molar (91 participants) and 17 mm - 43 mm in the second molar (74 participants) [40]. To allow tooth preparation, robots also need to have a sufficient operational workspace to access and treat the full dimensions of the targeted tooth. The maximum buccolingual width of human teeth is typically found in the first and second maxillary molars, measuring approximately 11 mm. In the mesiodistal dimension, the first mandibular molar exhibits the greatest width, also approximately 11 mm. The longest tooth is the central maxillary incisor, which has a cervicoincisal length of approximately 11 mm [34], [35]. In addition to the cervicoincisal length, some patients exhibit gingival recession, a condition in which the gum tissue retracts from the tooth, exposing the underlying root surface. This exposed root surface also needs to be prepared and covered by a restoration. The gingival recession typically ranges from 0 mm - 4 mm [36], [37], [38], [39], therefore, must be considered in the operational workspace of the MIR.

Based on these requirements of the tooth preparation procedure and anatomical constraints, the following robot design requirements were derived: robot's degrees of freedom (DoF), positioning accuracy, size, and operational workspace (Table I). In addition, the robot should incorporate a mechanism for actuating a dental bur (i.e., drill head). This drill head must be compact for use in the oral cavity.

B. Concept

We developed the following MIR concept based on the listed requirements. The MIR, equipped with a drill head for bur rotation, is designed to be mounted inside the oral cavity using a personalized fixation (bite block). The miniature intraoral robot can accurately guide a dental bur to perform tooth preparation. All functions required inside the oral cavity, including the robot's motion, bur rotation, and cooling, are provided through a flexible supply channel composed of multiple flexible tubes and shafts. Other components, such as the actuation unit including motors and the control unit, are externally located near the dental chair. For the rotation of a bur, a pneumatic-driven, turbine-based drill head was selected due to its compact size and the feasibility of actuation with flexible connections.

In this concept, only minimal components need to be placed inside the oral cavity, while larger, space-consuming units, such as motors, can be placed externally. This separation of units is beneficial in fulfilling the MIR's size requirements. Furthermore, local fixation of the MIR, combined with a flexible connection to external components, helps mitigate the propagation of mechanical disturbances between the external components and the MIR [31].

Therefore, this concept, featuring local fixation inside the oral cavity and a flexible supply channel, is expected to enable accurate bur positioning relative to the patient tissue. Its inherent mechanical decoupling from external components could potentially enhance robustness against disturbances such as patient motion, potentially eliminating the need for an external tracking system to detect unexpected relative motion between the patient and the robot. As a result, small patient movements could be potentially accepted without compromising accuracy and safety, which may contribute to improved patient comfort compared to setups where the head has to be fixed or the robot can only react in a delayed manner.

For the tooth preparation procedure, we defined two basic steps, involving at least one bur exchange (Fig. 3). The first step, occlusal height reduction, involves reducing the height of

TABLE II
MINIATURE INTRAORAL ROBOT DESIGN PARAMETERS

Miniature intraoral robot design			**Relevant information**
Degree of Freedom (DoF)		3 translational DoF of bur + bur rotation	
Workspace	X (mesiodistal direction)	> 12.3 mm	
	Y (buccolingual direction)	> 12.3 mm	
	Z (cervicoincisal direction)	9 mm	Bur exchange is required for full crown preparation.
Robot size	X (mesiodistal direction)	< 43 mm at the feed mechanism	
	Y (buccolingual direction)	< 26.4 mm at the feed mechanism	
	Z (cervicoincisal direction)	< 27.6 mm at the feed mechanism	Drill head height is 10 mm.

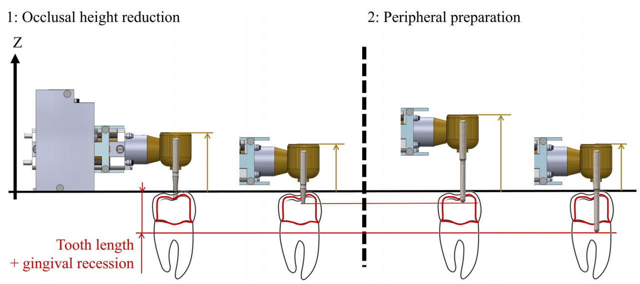

Fig. 3. Designed tooth preparation steps using the MIR. The first step can be performed using a shorter and larger diameter bur for occlusal height reduction (left). The second step involves peripheral preparation using a thinner and longer bur to reach the lower regions of the tooth and minimize the risk of contacting adjacent teeth (right).

the tooth by removing tooth substance at the occlusal surface. The second step, peripheral preparation, involves shaping the circumferential surface of the tooth. For the height reduction step, a relatively short bur with a relatively large diameter could be used to facilitate the efficient removal of tooth substance. The peripheral preparation step could be performed using a longer and thinner bur to access the lower regions of the tooth and to minimize the risk of unintentional contact with adjacent teeth. By dividing the tooth preparation procedure into two steps using different types of burs, the MIR can access a larger vertical range without extending its vertical actuation range. This approach enables a more compact robot design while still satisfying the vertical workspace requirements. Thus, the space required for the MIR's vertical motion can be adjusted by selecting an appropriate bur combination depending on the available space inside the patient's mouth.

III. IMPLEMENTATION

This section describes the prototype design implemented, its integration with the actuation components, and the control scheme.

A. Robot Design

The MIR consisted of two components: a parallel robot and a feed mechanism in the vertical direction (Fig. 4). The parallel robot, which can be equipped with a drill head and a bur, was designed to provide the planar positioning of a dental bur with three DoF (i.e., two translation and one rotation planar DoF). The feed mechanism was designed to allow vertical motion of the parallel robot, guiding the drill head and the bur. The implemented design parameters are summarized in Table II. The MIR prototype's parts were manufactured using Titanium grade 5 and stainless steel. The material pairings for the moving parts were selected to avoid contact between identical materials and to ensure compatibility with the required cleaning and autoclaving processes.

The movement of the robot was actuated via flexible shafts (Torque coil, Asahi Intecc Co., Japan) with an outer diameter of 1 mm and a hollow core (diameter of 0.3 mm) and a length of 250 mm. These flexible shafts were constructed of steel wire (SUS304) wound into coils, alternately twisted in three layers, and designed for transmitting bi-directional torques with a 1:1 torque transmission [46]. The torque transmission characteristics of the flexible shaft were experimentally evaluated under quasi-static and dynamic conditions. The results showed the flexible shaft exhibited an approximate 1:1 torque transmission ratio without delay over an angular speed range of 0 rad/s to 25 rad/s and a frequency range of 0 Hz to 4 Hz. An angular speed of 2.5 rad/s represents the average motors' angular speed employed in this study. The minimal bending radius of the flexible shafts was approximately 20 mm. These flexible shafts were connected to DC motors (Maxon Motor AG, Switzerland) with encoders (Maxon Motor AG, Switzerland) using stainless steel couplings. On the parallel robot side, the flexible shafts were connected to the leadscrews, which transformed the rotary motion of the motors into linear movements of the nuts and, therefore, of the parallel robot's joints. This parallel robot design was adapted from a miniature robot originally developed for laser bone cutting and modified to treat the larger workspace required for tooth preparation. Readers may refer to the previous publication for detailed information on the parallel robot's kinematics [29].

For actuating the feed mechanism, two flexible shafts were connected in parallel to worm gears (Shenzhen Minhong Technology Co., Ltd, China), which redirect the rotary motion by 90 degrees and transmitted the rotary motion to the leadscrews in a vertical direction. The two vertically oriented parallel lead screws and two vertical guide pins enabled vertical motion of a sliding frame. This sliding frame supported the parallel robot and provided vertical positioning. This feed mechanism provided a vertical motion range of 9 mm, ensuring adequate workspace for tooth preparation using two burs with different lengths. Both the parallel robot and the feed mechanism were designed to use over-actuated (redundant) leadscrew-based actuations. Redundant actuation in parallel robotics is known to be effective in reducing positioning error and improving stability by providing multiple actuation paths for the same motion [47], [48]. In addition, the leadscrews and the worm gears exhibit self-locking behavior, which offers resistance to back-driving. The back-driving resistance prevents external forces, such as gravitational forces or interaction forces during grinding, from moving the device unintentionally or from transmitting these forces back to the motors. This combination of redundant actuation and self-locking mechanisms is expected to enhance safety and accuracy while preventing unintended or uncontrolled motion through interaction forces.

The detailed design, including the size and workspace of the miniature intraoral robot, is summarized in Fig. 4. It was designed with minimal overall dimensions to fit inside

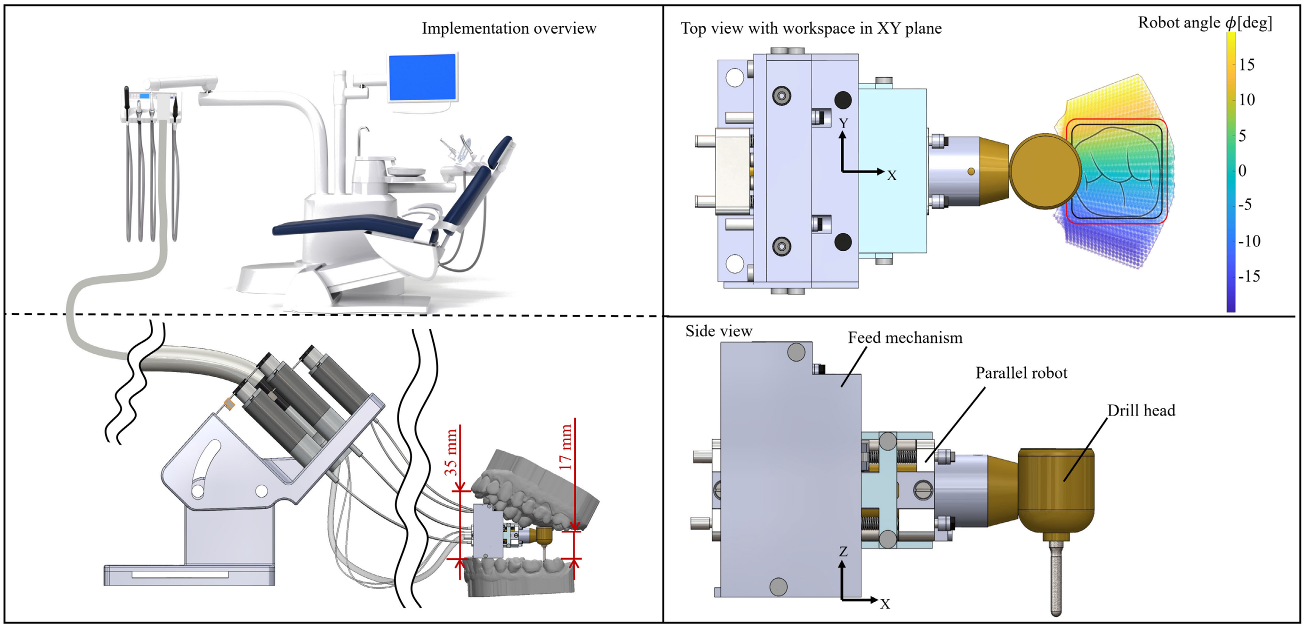

Fig. 4. The overview of the MIR's design and connection with a dental chair (top left). The MIR consisted of a feed mechanism allowing for the sliding frame, which holds the parallel robot with the drill head moving in the vertical direction (left bottom). The planar motion could be achieved by the parallel robot. The workspace was 12.3 mm in the x-direction, 12.3 mm in the y-direction, and 9 mm in the z-direction and met the requirements for tooth preparation (top right). The miniature intraoral robot consisted of the feed mechanism and the parallel robot with the drill head (right bottom).

the oral cavity. This design would fit inside the oral cavity with a mouth opening of around 18 mm at the second molar. The parallel robot provided a planar workspace around 12.3 mm x 12.3 mm, which is sufficient to treat the typical dimensions of molars (i.e., 11 mm in buccolingual direction and 11 mm in mesiodistal direction) with a bur diameter of 1.3 mm. The feed mechanism provided a vertical range of motion of 9 mm, allowing to treat a maximum tooth length of 11.7 mm with a gingival recession of 2.2 mm, using burs with the length ranging from 14 mm to 25 mm.

B. Drill Head Actuation and Cooling

The smallest commercially available turbine handpiece's drill head (NSK, Nakanishi Inc., Japan) was integrated into the MIR prototype using a 3D printed adapter. This drill head could accommodate commercial ISO-standard dental burs with friction grip (i.e., burs with ISO code numbers where the 4th and 5th digits are 31). Actuation of the burs was achieved using compressed air. The drill head included three channels: a compressed air channel for bur rotation, a compressed air channel for cooling, and a water channel for cooling. These channels were extended using silicone and polytetrafluoroethylene (PTFE) tubes and connected them to a coupling. This coupling enabled easy integration with a standard dental chair's turbine handpiece connection, allowing the miniature intraoral robot system to utilize the chair's compressed air and water cooling supplies. A modified dental chair's foot switch was connected to the centralized robot controller to allow compressed air and cooling supply activation through the miniature intraoral robot's controller (Fig. 4).

C. Calibration and Position Sensing

The position of the actuators inside the parallel robot (i.e., leadscrew and nut) was calibrated once by driving the nuts to their mechanical end-stops and defining these positions as the reference positions. Similarly, the positions of the actuators in the feed mechanism were measured using a vernier height gauge with 0.01 mm accuracy (Dial height gauge, Mitutoyo Corporation, Japan) and defined as the reference positions. The motor shaft positions were measured using encoders.

D. Control

A central controller unit, equipped with a real-time CPU module (Beckhoff AG) and motor drives (Maxon AG), enabled centralized control of the miniature intraoral robot's motion, bur rotation, and cooling functions with an update rate of 1 kHz. Motors' encoder positions were used to control the miniature intraoral robot. A position controller was used to move the robot through predefined paths in an open-loop scheme since there were no sensors, integrated measuring the absolute position of the miniature intraoral robot (Fig. 5). The miniature intraoral robot had 4-DoF for positioning a bur, consisting of three planar DoF of the parallel robot and one vertical DoF for the feed mechanism. The planar orientation of the robot (ϕ) was a redundant DoF for the grinding task and formed the null space. In an offline step, the desired Cartesian (3-DoF) path was augmented with a desired orientation using a null space selector. The null space selector sampled for all possible orientations in the workspace and selected the orientation that was farthest from kinematic singularities. The desired parallel robot pose on the planar path was converted to desired joint positions for the four joints ($q_1 - q_4$) using an analytical inverse kinematics solution (previously described in [29] for the parallel robot). The desired height for the feed mechanism (z_{des}) was directly mapped to the joint positions for the last two joints (q_5 and q_6). The desired joint positions were checked for the task space workspace position limits, velocity, and torque limits, and commanded to the low-level position controller on the motor drives. The measured joint positions by the motors' encoders were converted to the estimated robot pose with forward analytical kinematics (previously described

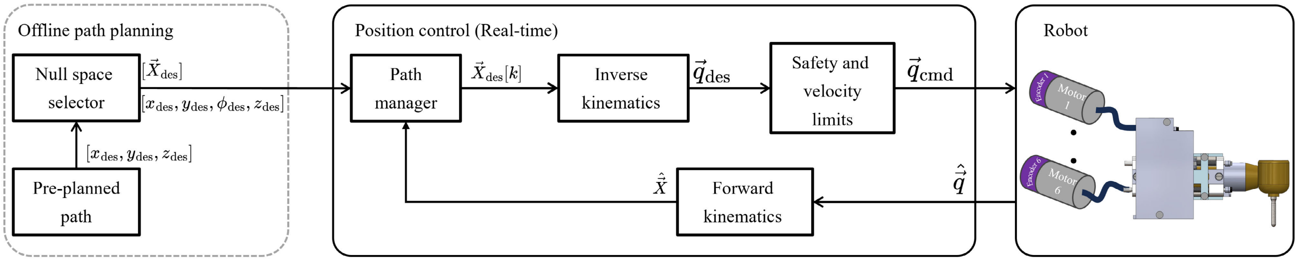

Fig. 5. Control overview to move the robot on a desired pre-planned path. In an offline path planning step, a point-wise 3-DoF path was iteratively sampled in the null space (ϕ) of the robot to include only feasible robot poses ($\vec{X}_{\text{des}}$). During real-time control, a position control scheme was used to command the robot through all the desired poses sequentially. The desired pose ($\vec{X}_{\text{des}}[k]$) was converted to desired joint positions ($\vec{q}_{\text{des}}$) using an analytical inverse kinematics solution. After verifying that the robot fulfills all the safety limits (position, velocity, torque), the commanded joint positions ($\vec{q}_{\text{cmd}}$) were sent to the motor drives. The motor drives were set to position control mode.

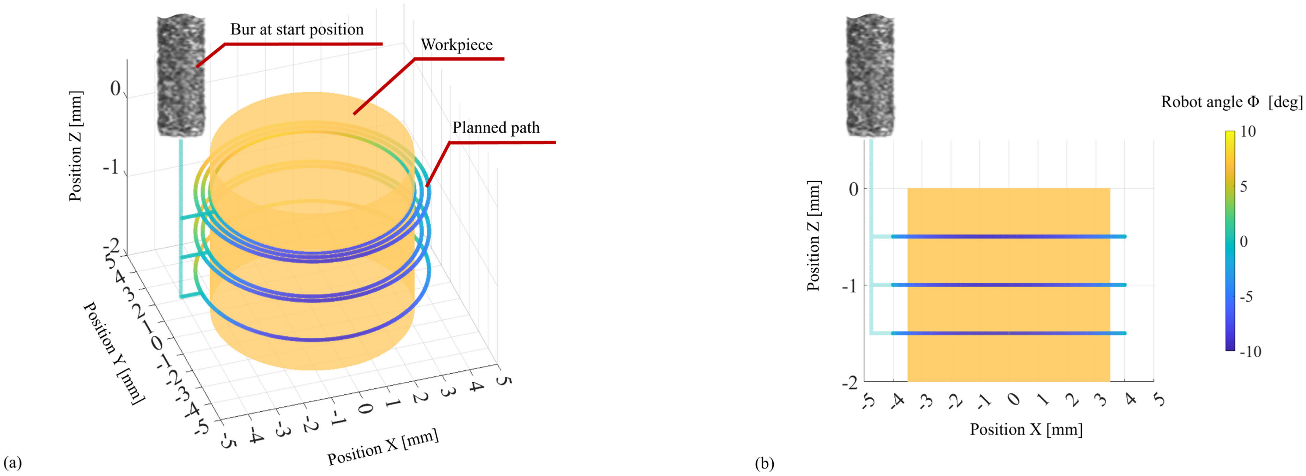

Fig. 6. A discrete conical path used in the experiments, shown with a workpiece and a bur tip in 3D view (a), and in side view (b). The path consisted of three layers, each composed of circular paths with different diameters. The miniature intraoral robot's angle (Yaw ϕ) along the path is represented by the color of the path. The discrete conical motion path started at the top of the cylindrical workpiece. The first layer consisted of three circular paths with decreasing diameters, each reducing the radius by 0.25 mm and cutting 0.5 mm deep into the material in the $z-$ direction. The first layer in this path resulted in a total radial material removal of 0.75 mm. The second layer consisted of two circular paths, spaced 0.25 mm apart in radius with a further 0.5 mm depth of cut. This second layer path resulted in a total radial material removal of 0.5 mm at a depth of 1.0 mm. The third layer consisted of a single circular path at the outermost diameter, completing the conical shape with material removal of 0.25 mm at the depth of 1.5 mm. Each circular path corresponds to a constant width of cut of 0.25 mm and a depth of cut of 0.5 mm, resulting in a stepped approximation of a conical profile.

[29] for the parallel robot). The path manager then moved to the next desired pose in the path when the error between the estimated and desired current robot poses was less than 0.01 mm in position and 2.5 ° in orientation.

IV. Experiments

A. Experimental Design

To evaluate the positioning and grinding functionalities of the miniature intraoral robot, experiments were carried out in two parts: 1) positioning accuracy evaluation experiment without grinding an object (i.e., no interaction forces in the bur) and 2) grinding performance evaluation experiment (i.e., including interaction forces in the bur). In both experiments, path-following experiments were performed in which the MIR was controlled to move along a predefined path with an average speed of 0.18 mm/s in the operational space. A discrete conical path (Fig. 6) was used to evaluate the path following and grinding performance required for tooth grinding in a simplified manner. The same path was used for both experiments. This discrete conical path consisted of circular motions with different diameters performed layer by layer. This path was generated to produce a stepped conical shape by grinding cylindrical workpieces with a diameter of 7 mm, using a defined set of grinding parameters, namely the diameter of the bur, the width of the cut, and the depth of the cut for each pass. Specifically, the path was generated for grinding with a bur diameter of 1.5 mm, a width of cut of 0.25 mm, and a depth of cut of 0.5 mm (in z-position) per circular path. These grinding parameters were selected based on preliminary tests to ensure that the grinding forces remained low enough (<2 N), thus avoiding excessive mechanical stress on the MIR.

B. Experimental Setup, Procedure and Data Analysis

All experiments were performed using the setup shown in Fig. 7. The experiment 1) *positioning accuracy evaluation* was performed without grinding an object; therefore, the workpiece and force torque sensor were removed from the setup. The experiment 2) *grinding performance evaluation* was performed with the force torque sensor and the grinding workpiece.

1) Positioning Accuracy Evaluation Experiment: The following procedure was used for the positioning accuracy evaluation experiment, and repeated three times. Before the experiments, the motion tracking system was calibrated using the calibration kit provided by the manufacturer. The miniature intraoral robot's bur tip was positioned at the starting position (Fig. 6 (a)), and subsequently, the path-following motion was

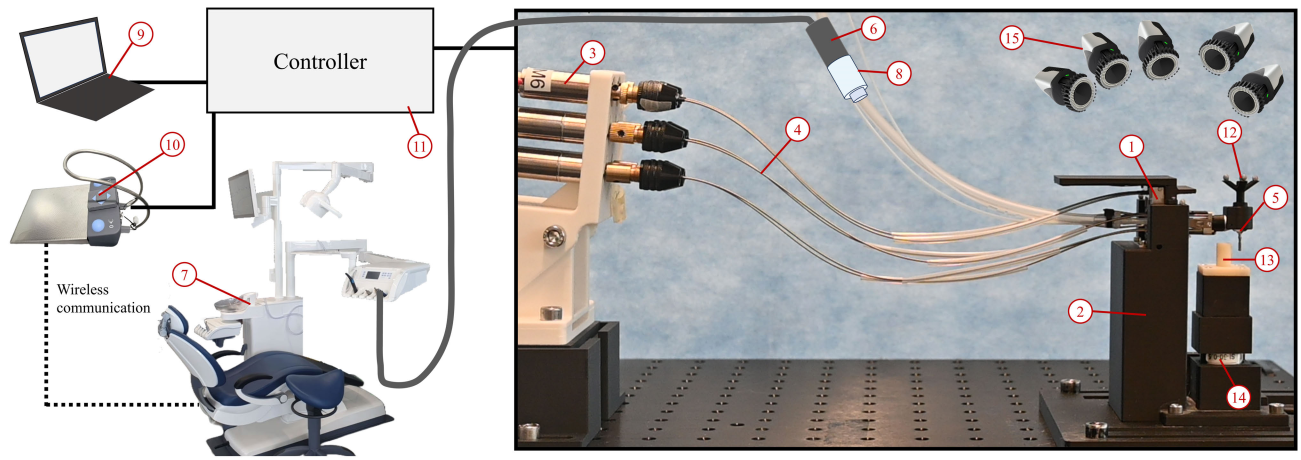

Fig. 7. Experimental setup with the prototype of the miniature intraoral robot (1). The miniature intraoral robot was fixed to the base by a 3D printed holder (2). The MIR's positioning mechanism was actuated by motors (3) connected by flexible shafts (4). The drill head (5) holding a bur on the miniature intraoral robot was connected to the turbine handpiece outlet (6) of the dental chair (7) via a coupling (8) for bur rotation and cooling. The developer computer (9) and the dental chair's foot switch (10) were connected to the miniature intraoral robot's central controller unit (11). The central controller unit, equipped with a real-time CPU module (Beckhoff AG), motor drives (Maxon AG), enabled centralized control of the miniature intraoral robot's motion, bur rotation, and cooling functions. Reflective markers were mounted on the miniature intraoral robot's drill head using a 3D printed marker holder (12). The grinding workpiece (13) was fixed above the force torque sensor (14) (Nano 17, ATI Industrial Automation), which was fixed to the base by the 3D printed holder. The position of the drill head was tracked using a motion capture system (15) (Qualisys AG). For the positioning accuracy evaluation experiment 1), the grinding workpiece and the force torque sensor were removed to allow the MIR's motion in the air without grinding.

activated to follow the predefined discrete conical motion path (Fig. 6) in the air. The miniature intraoral robot's drill head position was measured by tracking the position of the reflective markers attached to the drill head using a motion capture system (5 x Miqus M5, Qualisys, Sweden). The motion tracking data was recorded during the path following motion with Qualisys Track Manager (QTM) software (v2022.1, Qualisys, Gothenburg, Sweden) at a sample rate of 100 Hz.

The standard deviation of the wand length obtained from the calibration of the tracking system was 0.117 mm. The standard deviation of the distance measurements between the markers fixed on the drill head was smaller than 0.023 mm throughout the measurements. Thus, this measurement setup was considered sufficiently accurate.

2) Grinding Performance Evaluation Experiment: In the grinding performance evaluation experiment, a cylindrical workpiece of 7 mm diameter was ground layer by layer using the MIR prototype. Two types of workpiece materials were tested: a resin (SprintRay EU Temporary Crown & Teeth, SprintRay Europe GmbH, Germany) typically used for temporary crowns, and a dental hybrid ceramic (Vita Enamic, VITA Zahnfabrik H. Rauter GmbH & Co. KG, Germany) typically used for definitive crowns exhibiting a Vickers hardness closer to natural tooth enamel. The resin workpiece was made by additive manufacturing (SprintRay Pro S, SprintRay Europe GmbH), while the hybrid dental ceramic workpiece was made using a five-axis dental milling machine (Coritec One+, imes-icore GmbH). A coarse-grit diamond bur (FGM 204/10, Intensiv SA, Switzerland) with a total length of 16.5 mm, a working length of 3.9 mm, and a diameter of 1.5 mm was used. The force torque sensor (Nano 17 IP 68 with calibration SI-12-0.12, ATI Industrial Automation, USA) was placed below the workpiece to measure forces applied to the workpiece (grinding forces). The compressed air and water supply for the bur rotation and cooling of the miniature intraoral robot was provided by the dental chair (Sinius, Dentsply Sirona, USA). The air pressure for the bur rotation was set to 3 bar through the dental chair, which is a typical setting used for the actuation of a turbine handpiece. The modified dental chair's foot switch was interfaced with the robot's central controller to automate activation of the air and water supply without manual foot pedal activation. A rubber sheet was used to protect the MIR's mechanisms from debris and water. For the grinding experiments, the miniature intraoral robot was fixed to the base using a 3D printed holder. The workpiece was fixed to the force torque sensor mounted to the base using the 3D printed holder at a predefined location with respect to the robot. The cylindrical workpiece was registered by sequentially detecting its boundary before each grinding experiment. The robot was commanded to move first along the x−axis and subsequently along the z−axis, with each motion continuing until contact with the corresponding surface was detected by the force torque sensor. The midpoint of the x−ends was registered as the workpiece center, and the z−contact position was registered as the top of the workpiece. The robot was then moved to the starting position of the path.

The force torque sensor data was sent to the MIR's central controller and recorded at 1 kHz. After zeroing the force torque sensor, the path-following motion was activated. The bur rotation and cooling were activated throughout the path-following motion. The force torque data were recorded during the path-following motion. For the analysis of the grinding performance, the workpiece surface was scanned by a surface scanner (iMetric 4D, Imetric 4D Imaging, Courgenay, Switzerland) before and after the grinding experiment.

3) Data Analysis: All data were processed and analyzed in MATLAB R2023b (Mathworks Inc., USA). The bur tip position was calculated using the QTM software (v2022.1) based on the rigid body marker mounted on the drill head. This bur tip position was used for the evaluation of the positioning accuracy. The calculated bur tip position was zeroed at the start position of the discrete conical path during the data analysis. The bur tip position during the circular motion of the discrete conical path was used for the positioning error analysis. Two types of positioning error analysis were performed to evaluate the accuracy of the MIR motion: *a) positioning error relative* *to the preplanned circle* and *b) positioning error relative to the fitted circle*.

a) Positioning error relative to the preplanned circle: For each measured point in the circular path, the corresponding point in the planned circular path was determined by scaling the vector from the measured position to the center of the planned circle to match the radius of the planned circle. The positioning error was calculated as the Euclidean distance between the measured point and its corresponding point on the planned circular path, representing the absolute positioning errors from the planned circular path.

b) Positioning Error Relative to the Fitted Circle: A best-fit circle was estimated for each measured circular path by finding the center of the circle that minimized the sum of errors between the fitted circle and the measured points. Subsequently, the corresponding point in the fitted circle was determined for each measured point, and the positioning error was calculated with respect to the fitted circle using the same procedure used in Section IV-B3a) *positioning error relative to the preplanned circle*.

c) Grinding Surface Error Analysis: Grinding performance was evaluated by comparing STL surface data from the ground workpiece (i.e., actual data) and the planned ground surface (i.e., reference data) generated in Computer-Aided Design software (CAD) (SolidWorks, Dassault Systémes SolidWorks Corporation, USA), using ZEISS INSPECT (Carl Zeiss AG, Germany). The two surface data sets were aligned using a best-fit algorithm across the complete workpiece, and the error on the manually selected ground surface region was calculated using a function called "Create Surface Comparison on Actual" provided by the ZEISS INSPECT software. This function computed the perpendicular distance of each polygon point on the actual data to the reference data.

V. Results

A. Miniature Intraoral Robot (MIR)

The requirements for the miniature intraoral robot (MIR) were thoroughly analyzed, forming the basis for the development of its concept, design, and operational workflow. A first prototype was successfully manufactured, assembled, and commissioned for experiments on the test bench.

This MIR prototype was designed to feature three translational DoF and one rotational DoF for positioning of the bur, and one rotational DoF for bur rotation, providing sufficient DoF required for tooth preparation. In addition, the MIR prototype was designed to ensure the ability to prepare different types of teeth, even in their largest dimensions.

The entire MIR, including the drill head, fits inside a cuboid with the dimensions 43.0 mm × 26.4 mm × 27.6 mm. The drill head has a diameter of 8.6 mm and a height of 10 mm. The entire miniature intraoral robot can be mounted within a mouth opening of 18.2 mm in the second molar position, meeting the defined spatial requirements. The percentage of the population for whom the system is usable will vary depending on available bur lengths, location of the tooth to be prepared, and the preparation depth. Based on our planned workflow that includes up to one exchange of burs, we expect that we should achieve a coverage of 75% to 90% of the population, depending on which literature for the required gingival recession is taken into account and based on the measurements for mouth openings of 18.2 mm at the second molar performed at the the Clinic of Reconstructive Dentistry, University of Zürich (Section II-A. *Requirements*). [40]).

TABLE III
Error Between the Planned and Actual Circular Paths

	Circular path error [mm]	
	Mean	Max
Trial 1	0.17	0.46
Trial 2	0.18	0.46
Trial 3	0.18	0.47
All	0.18	0.47

TABLE IV
Error Between Fitted and Actual Circular Paths

	Circular path error [mm]		Circle center error [mm]	
	Mean	Max	Mean	Max
Trial 1	0.091	0.32	0.24	0.30
Trial 2	0.081	0.33	0.30	0.33
Trial 3	0.089	0.33	0.24	0.25
All	0.087	0.33	0.26	0.33

1) Positioning Accuracy Evaluation Experiment: A discrete conical path-following motion, which included a circular path with an 8 mm diameter, was performed. This experiment confirmed that the prototype is capable of covering a circular workspace of 8 mm in diameter, representing one example of the required workspace for tooth preparation. The position of the MIR's bur tip during the experiment in the first trial run is shown in Fig. 8. The results from Trials 2 and 3 are provided in the supplementary material. Two types of positioning error analyses were performed to evaluate the accuracy of the MIR's motion: *a) positioning error relative to the preplanned circle*, and *b) positioning error relative to the fitted circle* as described in IV-B3 *Data analysis*.

a) Positioning error relative to the preplanned circle: As a representative position measurement result using the optical tracking system, the measured bur tip position data is shown in (Fig. 8 (a). The circular paths in each layer are shown in the *xy*-plane together with the preplanned circular paths (Fig. 8 (b)-(d)). The positioning errors relative to the preplanned path for the circular paths were analyzed and summarized in Table III. The positioning errors with respect to the planned path resulted in an average error of 0.18 mm over the three trials, and a maximal error of 0.47 mm.

b) Positioning Error Relative to the Fitted Circle: As a representative example, measured, preplanned, and fitted circular paths are shown in Fig. 8 (d-2). The positioning errors relative to the fitted circular path are summarized in Table IV. The positioning errors with respect to the fitted circular path resulted in an average error of 0.087 mm, and a maximal error of 0.33 mm. The errors in the estimated circle centers were 0.26 mm on average, with a maximum error of 0.33 mm.

2) Grinding Performance Evaluation Experiment: The workpieces were ground using the discrete conical path as described in section IV-A. Grinding performance was evaluated by analyzing the measured grinding forces and the scans of the workpiece.

a) Grinding Force Analysis: The maximum grinding force applied on the workpiece was below 5 N throughout the grinding process, fulfilling the grinding force requirement.

b) Grinding Surface Error Analysis: The error between the planned ground shape and the actual ground shape of the workpiece is shown in Figure 9. The ground shape included an average absolute error of 0.176 mm for the resin workpiece and 0.176 mm for the dental hybrid ceramic (Vita Enamic) workpiece. The maximal absolute error was 0.593 mm for the

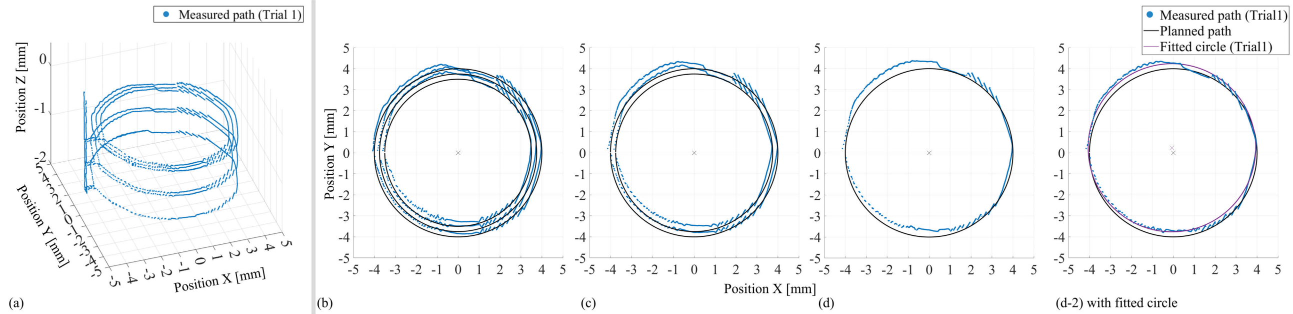

Fig. 8. Measured bur tip position of the MIR during the discrete conical path-following experiment (Trial 1). The measured position throughout the discrete conical path in 3D (a) and circular paths extracted from the discrete conical path plotted in the *xy*-plane (b-d). The cross marker indicates the center of the circle. The first layer consisted of three circular paths with progressively decreasing diameters (b), the second layer consisted of two circular paths (c), and the third layer consisted of a single circular path (d). The measured circular path is shown with the planned path and a fitted circle based on measured data, illustrating the three circular paths used for position error calculation in a representative example from the third layer of trial 1 (d-2). The results from Trials 2 and 3 are provided in the supplementary material.

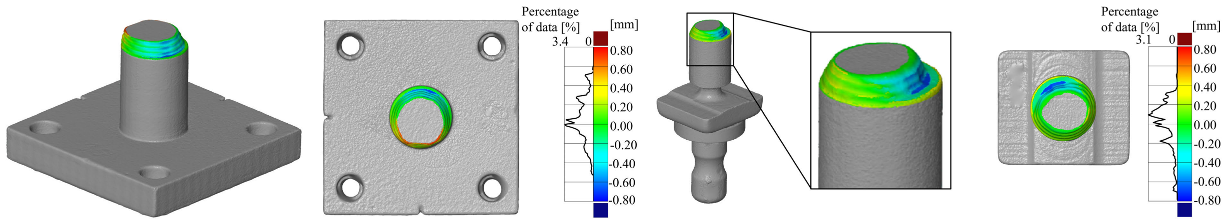

Fig. 9. Error between the planned mill surface and measured surface shown as a heat map projected on the 3D scan of two workpieces after grinding for resin (top) and dental hybrid ceramic (bottom) materials. The color map shows the distribution of the measured error. The results of the repetition grinding experiment for the resin workpiece (Trial 2) are provided in the supplementary material.

resin workpiece and 0.708 mm for the dental hybrid ceramic workpiece, respectively. The average error is 0.056 mm greater than the required positioning accuracy of 0.12 mm for the resin and the dental hybrid ceramic workpieces. The results of the repetitions of the grinding experiment for the resin workpiece (Trial 2) are provided in the supplementary material.

VI. Discussion

The first prototype of the MIR for tooth preparation was developed based on predefined requirements. The performance of this prototype was evaluated on the test bench using the path following experiments in the air and while grinding a cylindrical workpiece. We demonstrated that it is feasible to mill a discrete conical shape on the cylindrical workpiece with the MIR.

1) Design Requirements and Implementation:

We used the optical tracking system to evaluate the MIR's positioning accuracy during the experiments. However, optical tracking systems using reflective markers are not intended for use in a clinical application, as line-of-sight cannot be guaranteed inside the mouth.

In the current prototype, only the motors' encoders were used for position information, although direct absolute position measurements from the MIR are desirable in the future to ensure accurate and safe control. This sole reliance on motor encoder positions was due to the unavailability of commercial sensors suitable for direct integration into the MIR within the tight space constraints. However, in reality, transmission elements between the motors and the bur, such as flexible shafts, gears, and lead screws, can introduce errors due to transmission loss, elasticity, or backlash. In addition, other error sources, such as mechanical play and the effects of manufacturing tolerances, are also present. Detailed analysis of the contributors to the positioning errors is summarized in the literature for the parallel robot design [29]. To incorporate closed-loop control using direct position feedback for the MIR, it is required to develop and integrate a miniature sensing unit that can fit within the MIR in the future.

The MIR's prototype was manufactured with autoclave-compatible materials, i.e., titanium grade 5 and stainless steel. However, when electronic components such as sensors are integrated into the MIR in the future, the sterilization concept needs to be reassessed carefully. Encasing the MIR could be an alternative approach to autoclaving the entire device, which would also allow for the protection of the MIR's mechanical components, such as the lead screws, from machining debris.

2) Positioning Accuracy Evaluation Experiment:

The path-following motion with the discrete conical motion was successfully demonstrated, showing the basic feasibility of the three-dimensional motion required for tooth preparation. The average positioning error relative to the preplanned path was 0.18 mm on average over three trials, with a maximum error of 0.47 mm, showing the measured absolute accuracy did not yet fulfill the required positioning accuracy of 0.12 mm. However, positioning errors relative to the fitted circles averaged 0.087 mm, with a maximum of 0.33 mm, indicating that, while absolute precision was limited, consistency in following a circular path remained within the required accuracy range.

The maximum error observed was 0.47 mm relative to the pre-planned path, which is higher than the positioning accuracy requirements of 0.12 mm. The MIR was controlled using only the sensor data from the motor encoders, which are about 30 cm away from the MIR. Although further improvement in positioning accuracy is required, these results indicate that the first prototype of the MIR already operates in the order of magnitude of the error necessary for dental interventions. Potential improvements will therefore focus on including position sensors in the joints of the MIR and employing closed-loop control, which is expected to increase accuracy to the required level. Furthermore, fine-tuning the manufacturing tolerances is also expected to eliminate the remaining backlash in the mechanism, which will additionally contribute to further improving the positioning accuracy.

3) Grinding Experiment:

Cylindrical workpieces were ground with three layers of circles with different diameters. The ground workpieces exhibited a discrete conical shape with three steps, demonstrating the basic feasibility of layer-by-layer grinding at the submillimeter scale in resin and in dental hybrid ceramic that exhibits a Vickers hardness closer to natural tooth enamel.

In this report, experiments were performed on the test bench with firm fixations of the robot to the base using screws. The position of the workpiece was registered relative to the robot position using the force torque sensor for evaluation purposes in this experiment. We plan to develop a mechanical fixation block (i.e., bite block) for mounting the MIR inside the patient's mouth, which is expected to eliminate the need for the registration process. The robot showed that it is close to the desired performance requirements under the forces of interaction with the workpiece. The improvements previously suggested for including position sensors directly on the robot, which will allow closed-loop control, are expected to lead to the desired increase in positioning accuracy.

The MIR's performance with an average speed of 0.18 mm/s was tested as a first feasibility evaluation. In the future, a further performance evaluation with different grinding speeds is required to investigate their effect on the grinding performance and whether the entire tooth preparation can be performed in a reasonable time and with acceptable accuracy. In addition, further quantitative performance evaluation experiments in a condition closer to the real use case scenario, such as experiments inside a simulated intraoral environment considering neighboring teeth, different mouth opening, and other surrounding soft tissues, are required to understand the performance in the future. For example, a sensorized dental phantom head has recently been proposed to enable quantitative measurement of tooth preparation [49]. Such a platform could be leveraged for systematic benchmarking and further optimization of the MIR in the future. To advance toward automated full tooth preparation, several developments are still required, including digital ideal preparation designs relative to a defined restoration insertion axis and the generation of bur paths. Additionally, comprehensive evaluations of the preparation results on real teeth, such as assessments of surface roughness, temperature changes, and finish-line accuracy, will be essential to establish the performance and clinical applicability of the MIR.

VII. Conclusion

A miniature intraoral robot (MIR) concept was developed based on requirements derived from dental crown preparation procedures. The robot was then prototyped, commissioned, and evaluated on a test bench using path following experiments in air and during grinding of a cylindrical resin and dental hybrid ceramic workpieces. The results demonstrated submillimeter positioning accuracy and successful grinding of the workpiece. The feasibility of grinding workpieces using the prototyped MIR was shown on the test bench. Consistent circularity of the path was achieved with an average error of 0.087 mm, and an average absolute positioning error was 0.18 mm. This performance was achieved despite the absence of direct position feedback from the MIR and the sole reliance on the remote motor encoder positions in this experiment. Already at this initial stage of prototype evaluation, the robot is close to the desired accuracy required for the preparation of dental crowns. We expect that the integration of additional position sensors on the joints of the MIR will further improve positioning accuracy. With the implementation of the closed-loop control with the additional position sensors on the MIR, we believe that the positioning accuracy requirements for tooth preparation will be fully satisfied. Following the successful demonstration of grinding feasibility and grinding performance on the test bench, future work will include refining manufacturing tolerances, including direct position feedback from the MIR, and evaluating performance with realistic tooth geometries and materials in a setting closer to the actual oral cavity.

Acknowledgment

The authors thank Pibor ISO SA, Glovelier, Switzerland, for support in the prototype design and manufacturing, and Sascha Martin and his team at the Physics Workshop at the University of Basel, Switzerland. They also gratefully acknowledge the support of the Mechanical Design and Production Group, ARTORG Center for Biomedical Engineering, University of Bern, Switzerland, in the prototype design. They also thank Dr. Michael Sommerhalder for the technical support. They also gratefully acknowledge the support of the dental technicians of the Clinic of Reconstructive Dentistry, Center for Dental Medicine, University of Zürich. They also thank Intensiv SA, Collina d'Oro, Switzerland, for providing the burs that were used in the milling experiments. They also acknowledge the use of Grammarly, Writefull, and ChatGPT for grammar checks or paraphrasing. They have no conflict of interest to disclose.

References

[1] D. Edelhoff and J. A. Sorensen, "Tooth structure removal associated with various preparation designs for anterior teeth," *J. Prosthetic Dentistry*, vol. 87, no. 5, pp. 503–509, May 2002.

[2] D. Edelhoff and J. A. Sorensen, "Tooth structure removal associated with various preparation designs for posterior teeth," *Int. J. Periodontics Restorative Dentistry*, vol. 22, no. 3, pp. 241–249, 2002.

[3] J. Hjerppe, F. M. Rus, J. Pitta, S. von Felten, M. Ozcan, and G. Pradies, "Anterior full or partial coverage single tooth restorations—A systematic review of survival and complication rates," *Eur. J. Prosthodontics Restorative Dentistry*, early access, Sep. 2023.

[4] L. Zach and G. Cohen, "Pulp response to externally applied heat," *Oral Surg., Oral Med., Oral Pathol.*, vol. 19, no. 4, pp. 515–530, Apr. 1965.

[5] H.-C. Lauer, E. Kraft, W. Rothlauf, and T. Zwingers, "Effects of the temperature of cooling water during high-speed and ultrahigh-speed tooth preparation," *J. Prosthetic Dentistry*, vol. 63, no. 4, pp. 407–414, Apr. 1990.

[6] D. Y. Jung and Y. Jung, *Sleeve for Cutting Bur for Dental Cutting Guide*, U.S. Patent US 20 140,205 968 A1, Jul. 24, 2014.

[7] Y. Taha, F. Raslan, A. Ali, and M. Roig, "Guided tooth preparation device fabricated with a complete digital workflow: A dental technique," *J. Prosthetic Dentistry*, vol. 125, no. 2, pp. 1–4, Feb. 2021.

[8] M. Robles, C. A. Jurado, F. X. Azpiazu-Flores, J. Villalobos-Tinoco, K. I. Afrashtehfar, and N. G. Fischer, "An innovative 3D printed tooth reduction guide for precise dental ceramic veneers," *J. Funct. Biomaterials*, vol. 14, no. 4, p. 216, Apr. 2023.

[9] T. Otani, A. J. Raigrodski, L. Mancl, I. Kanuma, and J. Rosen, "In vitro evaluation of accuracy and precision of automated robotic tooth preparation system for porcelain laminate veneers," *J. Prosthetic Dentistry*, vol. 114, no. 2, pp. 229–235, Aug. 2015.

[10] Y. Li, Y. Zhou, J. Lyu, X. Cao, J. Tan, and X. Liu, "Feasibility and accuracy of semi-active robot-assisted porcelain veneer tooth preparation: An in vitro study," *J. Dentistry*, vol. 162, Nov. 2025, Art. no. 106012.

[11] J. Sun, J. Jiang, C. Wang, Z. Xue, A. Li, and J. Pan, "Trajectory optimization for tooth preparation robot based on P-MRSD algorithm," *IEEE Trans. Autom. Sci. Eng.*, vol. 22, pp. 13752–13763, 2025.

[12] J. Sun, J. Jiang, Z. Xue, J. Pan, and D. Qiao, "Layered preparation method for cracked tooth preparation robot based on iso-MRR algorithm," *IEEE/ASME Trans. Mechatronics*, vol. 30, no. 6, pp. 4411–4422, Dec. 2025.

[13] J. Sun, J. Jiang, Z. Xue, C. Wang, T. Shen, and J. Pan, "MC-CPO-based algorithm for collision-aware and preparation accuracy in confined space for tooth preparation robots," *IEEE Trans. Autom. Sci. Eng.*, vol. 23, pp. 1879–1892, 2026.

[14] J. Sun, J. Jiang, B. Ma, Y. Zhang, J. Pan, and D. Qiao, "Optimization of grinding parameters in robotic-assisted preparation of cracked teeth based on fracture mechanics: FEA and experiment," *Comput. Methods Programs Biomed.*, vol. 258, Jan. 2025, Art. no. 108485.

[15] C. Ciriello, G. Gallucci, P. Getto, J. Doeringer, J. Rosen, and K. Pala, "First in-human intervention using a semi-automated robot for tooth restorative treatment," *Res. Square*, Jun. 2025.

[16] *Meet Modern Dentistry*. Accessed: Jun. 11, 2025. [Online]. Available: https://www.perceptive.io/

[17] V. More et al., "Safety and performance of the first supervised automated dental robot to perform minimally invasive tooth prep for laminate veneers," *Int. J. Computerized Dentistry*, early access, Oct. 2025.

[18] (Feb. 2025). *Lupin Dental Announces First Clinical Use of Its Supervised Automated Robot*. [Online]. Available: https://www.surgicalroboticstechnology.com/news/lupin-dental-announces-first-clinical-use-of-its-supervised-automated-robot/

[19] J. Dong, S. Hong, and G. Hesselgren, "WIP: A study on development of endodontic micro robot," in *Proc. IJME-INTERTECH Conf.*, Oct. 2006, pp. 20104–20110.

[20] J. Dong and H. Everett, "The development of endodontic micro robot," in *Proc. Amer. Soc. Mech. Eng. Digit. Collection*, May 2009, pp. 201–204.

[21] J. Dong and S. Y. Hong, "Design of Z axis actuator and quick tool change assembly for an endodontic micro robot," in *Proc. Amer. Soc. Mech. Eng. Digit. Collection*, Apr. 2012, pp. 507–511.

[22] Y. Tao, N. Wu, S. Wang, Y. Li, W. Zhao, and W. Li, *Automatic Intraoral Operation Device for Dental Treatment*, CN Patent,CN 109 330,718 B, Dec. 12, 2023.

[23] A. Gleich, *Intraoral Dental Treatment Robot*, DE Patent DE 102 019 007 070 A1, May 14, 2020.

[24] S. Koubi and G. Gurel, *Intraoral Device for Automated Preparation of the Teeth With a View to Performing Partial or Peripheral Restorations*, U.S. Patent US 9 554 872 B2, Jan. 31, 2017.

[25] B. Mehdizadeh, *Systems and Methods for Performing Dental Operations*, U.S. Patent US20 050 084 816 A1, Apr. 21, 2005.

[26] A. Habib and O. Zouit, *Dental Devices*, CN Patent, CN 108 430 378 A, Aug. 21, 2018.

[27] D. K. Semenov, *Method for Precision Tooth Boring and Portable Unit with Remote Controlled Small-Size Tooth Boring Device*, RU Patent RU 2 443 396 C1, Feb. 27, 2012.

[28] F. Yuan, Y. Wang, Y. Zhang, Y. Sun, D. Wang, and P. Lyu, "An automatic tooth preparation technique: A preliminary study," *Sci. Rep.*, vol. 6, no. 1, p. 25281, Apr. 2016.

[29] M. Eugster, J.-P. Merlet, N. Gerig, P. C. Cattin, and G. Rauter, "Miniature parallel robot with submillimeter positioning accuracy for minimally invasive laser osteotomy," *Robotica*, vol. 40, no. 4, pp. 1070–1097, Apr. 2022.

[30] M. Eugster, P. Weber, and G. Rauter, *Medical Endodevice*, U.S. Patent US 11 617 495 B2, Apr. 4, 2023.

[31] Y. Tomooka, M. Karnam, M. Eugster, P. C. Cattin, and G. Rauter, "Disturbance propagation mitigation between a deployable miniature surgical robot and its insertion device," in *Advances in Mechanism and Machine Science (IFToMM WC 2023)*. Cham, Switzerland: Springer, 2023, pp. 800–809.

[32] Y. Tomooka, G. Rauter, N. Gerig, R. Takeda, P. Cattin, and M. Eugster, "Bending stiffness variability between a deployable robotic laser osteotome and its insertion device," *Current Directions Biomed. Eng.*, vol. 8, no. 1, pp. 138–141, Jul. 2022.

[33] P. M. Hjertton and M. Bågesund, "Er: YAG laser or high-speed bur for cavity preparation in adolescents," *Acta Odontologica Scandinavica*, vol. 71, nos. 3–4, pp. 610–615, Jan. 2012.

[34] P. Magne, G. O. Gallucci, and U. C. Belser, "Anatomic crown width/length ratios of unworn and Worn maxillary teeth in white subjects," *J. Prosthetic Dentistry*, vol. 89, no. 5, pp. 453–461, May 2003.

[35] S. J. Nelson, *Wheeler's Dental Anatomy, Physiology and Occlusion*. Amsterdam, The Netherlands: Elsevier, Dec. 2014.

[36] V. S. Yadav et al., "Global prevalence of gingival recession: A systematic review and meta-analysis," *Oral Diseases*, vol. 29, no. 8, pp. 2993–3002, Nov. 2022.

[37] C. Serrano, E. A. Suarez, and A. Uzaheta, "Prevalence and extent of gingival recession in a national sample of Colombian adults," *J. Int. Acad. Periodontology*, vol. 20, no. 3, pp. 94–101, Jul. 2018.

[38] I. Fragkioudakis, D. Tassou, M. Sideri, and I. Vouros, "Prevalance and clinical characteristics of gingival recession in Greek young adults: A cross-sectional study," *Clin. Experim. Dental Res.*, vol. 7, no. 5, pp. 672–678, Oct. 2021.

[39] M. Romandini, M. C. Soldini, E. Montero, and M. Sanz, "Epidemiology of mid-buccal gingival recessions in NHANES according to the 2018 world workshop classification system," *J. Clin. Periodontology*, vol. 47, no. 10, pp. 1180–1190, Oct. 2020.

[40] J. Hjerppe, J. Martin, A. N. Zuercher, R. Kraus, R. E. Jung, and M. Balmer, "Mouth Opening at Molar Regions: Clinical Assessment of the Accessibility in the Posterior Dental Area—A Cross-Sectional Study," *Int. J. Prosthodontics*, 2026.

[41] H. T. Shillingburg and D. A. Sather, *Fundamentals of Fixed Prosthodontics*, vol. 194. Chicago, IL, USA: Quintessence Publishing Company, 1997.

[42] G. Liu, Y. Zhang, and W. T. Townsend, "Force modeling for tooth preparation in a dental training system," *Virtual Reality*, vol. 12, no. 3, pp. 125–136, Sep. 2008.

[43] S. Suebnukarn, N. Phatthanasathiankul, S. Sombatweroje, P. Rhienmora, and P. Haddawy, "Process and outcome measures of expert/novice performance on a haptic virtual reality system," *J. Dentistry*, vol. 37, no. 9, pp. 658–665, Sep. 2009.

[44] L. Cho, H. Song, J. Koak, and S. Heo, "Marginal accuracy and fracture strength of ceromer/fiber-reinforced composite crowns: Effect of variations in preparation design," *J. Prosthetic Dentistry*, vol. 88, no. 4, pp. 388–395, Oct. 2002.

[45] K. B. May, M. M. Russell, M. E. Razzoog, and B. R. Lang, "Precision of fit: The procera AllCeram crown," *J. Prosthetic Dentistry*, vol. 80, no. 4, pp. 394–404, Oct. 1998.

[46] *Torque Coil*. Accessed: Oct. 27, 2025. [Online]. Available: https://filmecc.com/en/medical-part/product/torque-coil/

[47] J.-P. Merlet, *Parallel Robots*, vol. 128. Berlin, Germany: Springer, 2006.

[48] S. Fang, *Modeling and Motion Control of Tendon Based Parallel Manipulators*. Düsseldorf, Germany: VDI-Verlag, 2005.

[49] C. Schmidt et al., "Sensorized dental phantom: Enabling in-depth analysis of tooth preparation in a realistic setting," Apr. 2026.